THE ASTROPHYSICAL JOURNAL, 387:276–287, 1992 March 1

VORTEX DRAG AND THE SPIN-UP TIME SCALE FOR PULSAR GLITCHES

RICHARD I. EPSTEIN AND GORDON BAYM[1]
Los Alamos National Laboratory, MS D436, Los Alamos, NM 87545
Received 1991 May 20; accepted 1991 August 20

ABSTRACT

We investigate the coupling of the superfluid of a neutron star with the solid crust arising from the scattering of individual nuclei in the inner crust with dynamical vortex lines of the superfluid. Such interactions generate quantized Kelvin mode vortex oscillations (*kelvons*). We calculate the rate of kelvon production and the consequent drag produced on the superfluid. The coupling is sufficiently strong to permit glitch spin-up time scales $\lesssim 60$ times the rotation period. Catastrophic vortex-unpinning events are therefore capable of producing giant glitches with rapid spin-ups on the scale observed in the Vela pulsar.

Subject headings: stars: neutron — stars: pulsars: general

1. INTRODUCTION

In the inner crust of a neutron star a gas of free neutrons coexists with a lattice of neutron-rich nuclei. For stellar densities $\sim 10^{12}$–10^{14} g cm^{-3}, corresponding to free neutron densities $\sim 10^{-3}$–10^{-1} fm^{-3}, the free neutrons are believed to pair and form an isotropic s-wave superfluid. In a rotating star the neutron superfluid rotates by forming vortex lines, singular regions in which the superfluidity vanishes and around which the superfluid circulation is $\kappa = \pi\hbar/m_n$, where m_n is the neutron mass. The superfluid velocity in the neutron star is completely determined by the spatial arrangement of the vortex lines. A change in the velocity field requires a corresponding change in the vortex line distribution, either a distortion of the configuration of the existing lines or creation of new lines.

Some of the peculiar variations in the rotation rates of isolated, rotation-powered pulsars are attributed to interactions of the normal (nonsuperfluid) parts of the stars with the neutron superfluid in the inner crust. Anderson & Itoh (1975) suggested that a pulsar glitch, the rapid spin-up of the crust of the star, is due to the sudden transfer of angular momentum from the superfluid to the solid crust. Giant glitches are rotational accelerations of order $\Delta\Omega_c/\Omega_c \sim 10^{-6}$, observed to last less than 2 minutes, where Ω_c is the observed rotation rate of the crust and $\Delta\Omega_c$ is its change (Manchester & Taylor 1977; Hamilton, King, & McCulloch 1989).

A physical explanation of pulsar timing observations entails describing the coupling mechanism by which angular momentum is transferred between the crust and the superfluid. Among the several processes that contribute to this coupling (Feibelman 1971; Bildsten & Epstein 1989; Jones 1990), the most important one appears to be the excitation of waves on a vortex line by interaction with nuclei in the crust. As a vortex line moves past nuclei, the vortex-nucleus interaction bends and twists the vortex line and pulls the nuclei away from their equilibrium positions in the crystal lattice of the crust. These perturbations excite quantized Kelvin mode oscillations—or *kelvons*—on the vortex line and phonons in the crystal. The properties of kelvons are reviewed in Appendix A. Interactions between acoustic phonons in the crystal lattice and kelvons tend to bring the vortex excitations into thermal equilibrium with the solid crust. In this paper we focus on the generation of kelvons by the relative motion of a vortex line and nuclei; this process creates a drag on vortex lines and is one of the dominant coupling mechanisms between the superfluid and the crust.

This paper is organized as follows: § 2 gives estimates of the vortex-nuclear interaction and the impulse on a moving vortex line. Section 3 presents the calculation of the drag on a vortex line and the rate for generating quantized vortex excitations. Section 4 discusses the relationship between the pinning and dynamics of vortex lines and the overall dynamics of the superfluid. Section 5 summarizes the main results and relates them to observations of pulsar glitches. Appendix A describes vortex-line excitations as classical waves and as quantum excitations, Appendix B presents a calculation of the Fourier transform of the vortex-nucleus force, and Appendix C gives a classical derivation of the energy imparted to vortex excitations by a single vortex-nucleus interaction.

2. INTERACTION BETWEEN A VORTEX LINE AND A NUCLEUS

To begin the discussion of encounters between nuclei and vortex lines, we first treat the interaction of a single nucleus with a vortex line. In Epstein & Baym (1988, hereafter Paper I) we estimated the interaction energy $E_{\rm int}(s)$ between a nucleus and a vortex line as a function of their separation s. For stellar densities between $\sim 7 \times 10^{11}$ and 10^{14} g cm^{-3}, $E_{\rm int}(s)$ can be approximated by

$$E_{\rm int}(s) = \frac{E_S}{(1 + s^2/R^2)^4} + \frac{E_L}{1 + s^2/R^2}\,, \qquad (2.1)$$

plus terms independent of s. Here R is the effective nuclear radius, E_S is the energy related to the *short*-range part of the interaction, and E_L is related to the *long*-range repulsion; while E_L is always positive, E_S can be positive or negative depending on density. From equation (2.1) one finds that the total force on the vortex line is

$$\begin{aligned} \boldsymbol{F}_{\rm int} &= -\nabla_s E_{\rm int}(s) \\ &= \frac{2s}{R^2}\left[\frac{4E_S}{(1 + s^2/R^2)^5} + \frac{E_L}{(1 + s^2/R^2)^2}\right] \end{aligned} \qquad (2.2)$$

[1] Also Loomis Laboratory of Physics, University of Illinois, 1110 W. Green Street, Urbana, IL 61801.

(we use the convention that upper-case $\boldsymbol{F}$ represents a total force, and lower-case $\boldsymbol{f}$ represents a force per unit length). Table 1 gives values of R, E_S, and E_L from Paper I as functions of the total matter density ρ_* (including the neutron superfluid, nuclei, electrons, etc.) in the inner crust.

The values of E_S in Table 1 are uncertain since a fully microscopic treatment of the short-range component of the vortex-nucleus interaction is not yet available. For densities above $\sim 10^{14}$ g cm^{-3}, the interaction energy derived in Paper I has a more complicated dependence on s than that of equation (2.2) because the superfluid in the nuclei undergoes a phase transition to the normal state as the nucleus approaches a vortex line; for these densities we will use equation (2.2) with E_S adjusted to give the correct maximum force. Upper limits on the internal heating in neutron stars due to vortex creep, inferred from neutron star surface temperatures, suggest that the values of E_S estimated in Paper I may be too large (Shibazaki & Lamb 1989); to allow for this possibility, we will also consider the consequences of lower E_S. Since the long-range interaction is largely due to hydrodynamic effects, the values of E_L are more certain.

To calculate the dynamics of a vortex line passing a nucleus, one needs the interaction force on the nucleus per unit length of vortex. Consider a Cartesian coordinate system in the rest frame of the vortex line with $\hat{z}$-axis coincident with the vortex line. For a nucleus at $(x, y, 0)$ we write the interaction force between an element of length dz of the vortex line at z and the nucleus in the form

$$\boldsymbol{f}_{\text{int}}\, dz = \boldsymbol{F}_{\text{int}}(\boldsymbol{s})\phi(z, s)dz \,, \tag{2.3}$$

where $\boldsymbol{s} \equiv \boldsymbol{x} + \boldsymbol{y}$, $s = |\boldsymbol{s}|$, and $\phi(z, s)$ is the normalized distribution of the interaction force along the vortex line,

$$\int_{-\infty}^{\infty} \phi(z, s)dz = 1 \,. \tag{2.4}$$

For the physical processes of interest in this paper we will not, in fact, need to specify the precise form of ϕ.

We take the relative velocity $\Delta\boldsymbol{v}$ of the nucleus past the vortex to be in the x-direction. For small energy transfers, the nuclear trajectory is nearly straight,

$$\boldsymbol{s}(t) = \Delta v t\hat{x} + b\hat{y} \,, \tag{2.5}$$

where b is the nucleus-vortex impact parameter. In addition, if the vortex line remains essentially straight as the nucleus passes, the nucleus imparts a total force (eq. [2.2]), and a force per unit length on the vortex line,

$$\boldsymbol{f}_{\text{int}}(z, t) = \frac{2(\tau\hat{x} + \tau_b\hat{y})}{R} \times \left[\frac{4E_S}{(1 + \tau^2 + \tau_b^2)^5} + \frac{E_L}{(1 + \tau^2 + \tau_b^2)^2}\right]\phi[z, s(t)] \,, \tag{2.6}$$

where $\tau \equiv \Delta v t/R$ is the dimensionless time, $\tau_b \equiv b/R$, and $s(t)/R = (\tau^2 + \tau_b^2)^{1/2}$. As discussed in § 4, the force (eq. [2.6]) is valid as long as the relative velocity Δv is not too small.

TABLE 1

VORTEX-NUCLEUS INTERACTION PARAMETERS

$\log \rho_*$ (g cm^{-3})	R (fm)	E_S (MeV)	E_L (MeV)	$\log \rho_s$ (g cm^{-3})	$\log n_N$ (fm^{-3})	l_i (fm)
11.83......	5.7	2.5	0.037	11.21	−5.70	4900
11.99......	5.8	3.3	0.090	11.63	−5.62	3900
12.18......	5.9	4.2	0.16	11.90	−5.56	3300
12.41......	6.1	6.3	0.34	12.30	−5.50	2700
12.79......	6.5	7.5	0.72	12.70	−5.41	1900
12.98......	6.7	−1.3	0.94	12.89	−5.28	1400
13.18......	6.9	−7.7	1.3	13.11	−5.18	1000
13.53......	7.2	−16.4	1.4	13.48	−4.95	540
13.89......	7.3	−10.0	1.0	13.86	−4.50	190
14.12......	7.2	−7.8	0.49	14.09	−4.10	76

3. EXCITATION OF VORTEX OSCILLATIONS

We now consider the effects of small local displacements of the vortex line on its interaction with nuclei. We write the displacement of the line from its equilibrium position as

$$\boldsymbol{\epsilon}(z, t) = \epsilon_x(z, t)\hat{x} + \epsilon_y(z, t)\hat{y} \,. \tag{3.1}$$

With displacement (3.1), a point on the vortex line is at position $\boldsymbol{r}_v(z, t) = \boldsymbol{z} + \boldsymbol{\epsilon}(z, t)$, where $\boldsymbol{z} = (0, 0, z)$, and the vector $\boldsymbol{w}$ between this point and the position of the nucleus (eq. [2.5]) is

$$\boldsymbol{w}(z, t) \equiv \boldsymbol{s}(t) - \boldsymbol{r}_v(z, t) = \boldsymbol{w}_0(z, t) - \boldsymbol{\epsilon}(z, t) \,, \tag{3.2}$$

where $\boldsymbol{w}_0(z, t) \equiv \boldsymbol{s}(t) - \boldsymbol{z} = \Delta v t\hat{x} + b\hat{y} - \boldsymbol{z}$. Expanding the interaction energy of the vortex line, $H_{\text{int}}(t) = \int dz V(\boldsymbol{w})$, in powers of $\boldsymbol{\epsilon}$, we obtain

$$H_{\text{int}}(t) = \int_L dz[V(\boldsymbol{w}) - \boldsymbol{\epsilon} \cdot \nabla V(\boldsymbol{w}) + \tfrac{1}{2}(\boldsymbol{\epsilon} \cdot \nabla)^2 V(\boldsymbol{w}) + \cdots]_{\boldsymbol{w}=\boldsymbol{w}_0(t)} \,, \tag{3.3}$$

where L is the total length of the vortex line. The first term in the expansion describes the adiabatic interaction between the nucleus and the vortex line with no energy transferred to the line. The expression linear in $\boldsymbol{\epsilon}$ is the lowest-order term in $H_{\text{int}}(t)$ that transfers energy to the vortex line, and it is an important, and possibly the dominant, term for exciting vortex lines and damping vortex motion.[2] This linear term represents a dissipative process that converts the free energy of the differential motion between the superfluid and the nuclei in the crust into vortex excitations, and as shown below tends to increase the number of kelvons. The number of vortex excitations cannot, however, increase indefinitely. If the vortex excitations become effectively "hotter" than the phonons in the nuclear lattice, then kelvon-phonon processes preferentially destroy kelvons, create phonons, and heat the crust. These processes are treated in a subsequent paper.

We write the first-order term in $H_{\text{int}}(t)$ in terms of the interaction force (eq. [2.6]) as

$$H_{\text{int}}^{(1)}(t) = \int_L dz\, \boldsymbol{\epsilon}(z, t) \cdot \boldsymbol{f}_{\text{int}}(z, t) \,, \tag{3.4}$$

with $\boldsymbol{f}_{\text{int}} = -\nabla V(\boldsymbol{w})_{\boldsymbol{w}_0}$. As described in Appendix A, the displacement $\boldsymbol{\epsilon}(z, t)$ can be expressed in terms of creation and annihilation operators, $a_k^\dagger$ and a_k, for kelvons of wavenumber k:

[2] Jones (1990) ignores this term claiming, contrary to our arguments here, that it does not generate a net increase in the number of vortex excitations.

$$\epsilon(z, t) = \left(\frac{\hbar}{\rho_s \kappa L}\right)^{1/2} \sum_k [a_k e^{ikz}\boldsymbol{\lambda} + a_k^\dagger e^{-ikz}\boldsymbol{\lambda}^*] . \tag{3.5}$$

Here $\boldsymbol{\lambda}$ is the (left) circular polarization unit vector for a kelvon,

$$\boldsymbol{\lambda} = \frac{\hat{x} - i\hat{y}}{\sqrt{2}} , \tag{3.6}$$

ρ_s is the superfluid mass density, and the asterisk denotes the complex conjugate. The frequency of a kelvon is given by

$$\omega_k = \frac{\hbar k^2}{2\mu} , \tag{3.7}$$

where

$$\mu = \frac{m_n}{\pi \Lambda(k)} . \tag{3.8}$$

The dimensionless parameter Λ is given by $\Lambda \simeq 0.116 - \ln(k\xi)$ for "hollow core" vortex lines with wavenumbers in the range $d_v^{-1} \ll k \ll \xi^{-1}$, where d_v is the spacing between vortex lines and ξ is the size of the vortex core. In the inner crust $\xi \sim 10$ fm, and the intervortex spacing is $d_v \gtrsim 10^{-3}$ cm. The above form for Λ is thus valid for 10^{-10} fm$^{-1} \ll k \ll 10^{-1}$ fm^{-1}, a condition well satisfied for the excitations of importance.

Expressions (3.5) and (3.7) neglect the interactions among vortices and Coriolis effects. Tkachenko (1965, 1966, 1969) (see also Baym & Chandler 1983; Chandler & Baym 1986) examined the oscillations of superfluids including the effects of the vortex lattice and showed that the elasticity of the vortex lattice produce collective oscillations (Tkachenko modes) with frequencies up to approximately the superfluid rotation rate. Neutron star rotation frequencies, below $\sim 10^4$ s^{-1}, are negligible compared to the relevant kelvon frequency, $\omega_k \sim 10^{17}$ s^{-1}, corresponding to $k \sim 10^{-3}$ fm^{-1}; see equation (3.20) below. Thus vortex interactions and Coriolis terms can be ignored here.

Substituting expression (3.5) for ϵ in the Hamiltonian (3.4), we find

$$H_{\rm int}^{(1)}(t) = \left(\frac{\hbar}{\rho_s \kappa L}\right)^{1/2} \int_L dz \sum_k [a_k e^{ikz}\boldsymbol{\lambda} \cdot \boldsymbol{f}_{\rm int}(z, t) + a_k^\dagger e^{-ikz}\boldsymbol{\lambda}^* \cdot \boldsymbol{f}_{\rm int}(z, t)] . \tag{3.9}$$

The net number of kelvons of wavevector k created in a vortex line as a nucleus passes is the difference in the number created by the $a_k^\dagger$ term and the number annihilated by the a_k term in equation (3.9). If the initial state contains n_k kelvons of wavenumber k, first-order perturbation theory gives the probability that a kelvon of wavenumber k is created in collision as

$$P_{n_k \to n_k+1} = \frac{1}{\hbar^2} \left| \int_{-\infty}^{\infty} dt e^{i\omega_k t} \langle n_k + 1 | H_{\rm int}^{(1)}(t) | n_k \rangle \right|^2 = \frac{n_k + 1}{\hbar \rho_s \kappa L} | f_+(k, \omega_k) |^2 , \tag{3.10}$$

and the probability that a kelvon is annihilated as

$$P_{n_k \to n_k-1} = \frac{n_k}{\hbar \rho_s \kappa L} | f_+(k, \omega_k) |^2 , \tag{3.11}$$

where

$$f_+(z, t) \equiv \boldsymbol{f}_{\rm int}(z, t) \cdot \boldsymbol{\lambda}^* , \tag{3.12}$$

and $f_+(k, \omega_k)$ is its spacetime Fourier transform.[3]

With each interaction the number of kelvons of wavenumber k thus increases by

$$\Delta n_k = \frac{1}{\hbar \rho_s \kappa L} | f_+(k, \omega_k) |^2 , \tag{3.13}$$

independent of the initial occupation number. The total energy transferred to the vortex line per scattering is

$$E_{\rm scatt}(b) = \sum_k \hbar\omega_k \Delta n_k = \frac{\hbar}{2\rho_s \kappa \mu L} \sum_k k^2 | f_+(k, \omega_k) |^2 , \tag{3.14}$$

which in the continuum limit, $L \to \infty$, becomes

$$E_{\rm scatt}(b) = \frac{\hbar}{4\pi \rho_s \kappa \mu} \int_{-\infty}^{\infty} | f_+(k, \omega_k) |^2 k^2 \, dk . \tag{3.15}$$

In Appendix C we obtain this result alternatively by solving the classical equations for exciting vortex oscillations.

The power dissipated per length of vortex line due to scattering with nuclei of number n_N per unit volume is

$$p_d = n_N \Delta v \int_{-\infty}^{\infty} E_{\rm scatt}(b) db , \tag{3.16}$$

where b is the impact parameter. Using the Fourier transform $f_+(k, \omega_k)$ given by equation (B14) in Appendix B, we numerically evaluate integral (3.16) to obtain

$$p_d = \rho_s \kappa (\Delta v)^{1/2} v_*^{3/2} , \tag{3.17}$$

where

$$v_* \simeq 9.9 \left(\frac{n_N^2 \mu}{\rho_s^4 \kappa^4 \hbar R}\right)^{1/3} (E_S^2 + 0.75 E_S E_L + 0.27 E_L^2)^{2/3} \tag{3.18}$$

is a characteristic velocity for the vortex dynamics (see § 4). Table 2 gives computed values of v_* in the inner crust for two sets of values of the short-range interaction energy E_S: the full value of E_S given in Table 1 and this value reduced by a factor of 10. The physical parameters in equation (3.18) are taken from Negele & Vautherin (1973) and Paper I. The logarithmic factor, Λ, in the definition (3.8) of μ is evaluated at $k_*(v_*)$ (see eq. [3.20]). The $(\Delta v)^{1/2}$ dependence in the dissipation rate is

[3] We use the following normalization conventions for the Fourier transforms:

$$A(t) = \int_{-\infty}^{\infty} \frac{d\omega}{2\pi} e^{-i\omega t} A(\omega) , \quad A(\omega) = \int_{-\infty}^{\infty} dt e^{i\omega t} A(t)$$

$$B(z) = \frac{1}{L} \sum_k e^{ikz} B(k) , \quad B(k) = \int_{-L/2}^{L/2} dz e^{-ikz} B(z) ,$$

where the vortex line is of length L and we use periodic boundary conditions at $\pm L/2$. The summation is over $k = 2\pi n/L$, $n = 0, \pm 1, \pm 2, \ldots$.

TABLE 2

PARAMETERS FOR THE VORTEX DYNAMICS

	FULL E_S		REDUCED E_S			
$\log \rho_*$ (g cm^{-3})	$\log v_*$ (cm s^{-1})	$\log v_B$ (cm s^{-1})	$\log v_*$ (cm s^{-1})	$\log v_B$ (cm s^{-1})	$\log v_{\min}$ (cm s^{-1})	$\log k_*(v_*)/\Delta v_7^{1/2}$ (fm^{-1})
11.83......	8.55	5.15	7.14	5.15	4.25	−2.01
11.99......	8.16	5.20	6.80	5.20	4.43	−2.08
12.18......	7.97	5.28	6.63	5.28	4.58	−2.10
12.41......	7.69	5.32	6.39	5.32	4.76	−2.14
12.79......	7.29	5.43	6.08	5.43	5.06	−2.19
12.98......	5.88	7.20	5.33	6.20	5.36	−2.29
13.18......	6.82	8.20	5.27	7.20	5.60	−2.24
13.53......	6.94	8.23	5.40	7.23	6.11	−2.24
13.89......	6.41	7.72	4.86	6.72	6.94	−2.28
14.12......	6.24	7.58	4.74	6.58	7.62	−2.28

readily understood by looking at expressions (3.16) and (3.14). The dissipation rate is proportional to Δv times $E_{\rm scatt}$, and $E_{\rm scatt}$ is proportional to the product of the characteristic frequency ω that is excited, the effective bandwidth $\Delta k \propto \omega^{1/2}$, and the square of the matrix element. Taking the characteristic frequency to be $\omega \sim \Delta v/R$, where R is the effective nuclear radius, and the matrix element to be $\propto 1/\Delta v$, as in equation (B2), one has $p_d \propto (\Delta v)^{1/2}$.

The above derivation assumes that each interaction between a vortex line and a nucleus is distinct and that the excitations from each interaction add incoherently on average. If the characteristic wavelength of excitations is comparable to the distance l_i between two points that are being plucked at one time, one cannot treat the two interactions as independent. To estimate l_i we assume that all nuclei that lie within a distance $\sim R$ of a vortex line interact with the line. If the vortex line is of length L, the number of nuclei interacting with the line at any instant is $N \sim \pi R^2 L n_N$, and

$$l_i = \frac{L}{N} \sim \frac{1}{\pi R^2 n_N} . \tag{3.19}$$

For a given velocity difference Δv the characteristic wavenumber for the excitation spectrum is

$$k_*(\Delta v) \equiv (2\mu\,\Delta v/\hbar R)^{1/2} , \tag{3.20}$$

and a necessary condition for the excitations from different encounters to be independent is that

$$l_i k_*(\Delta v) \gg 1 , \tag{3.21}$$

or equivalently,

$$\Delta v \gg v_{\min} \equiv \frac{\hbar R}{2\mu l_i^2} . \tag{3.22}$$

Table 2 shows values of $v_{\min}$ at several densities in the inner crust.

The rate at which vortex excitations are generated along the total length of a given line is

$$\frac{\partial n_k}{\partial t} = n_N \Delta v L \int_{-\infty}^{\infty} \Delta n_k \, db = \frac{n_N \Delta v R}{\hbar \rho_s \kappa} \int_{-\infty}^{\infty} |f_+(k, \omega_k)|^2 \, d\tau_b , \tag{3.23}$$

with $\tau_b = b/R$. Using the transform (B14) we find that in the limits of small and large k the rate (eq. [3.23]) is

$$\frac{\partial n_k}{\partial t} = 0.974 \frac{n_N R}{\hbar \Delta v \rho_s \kappa} \times \begin{cases} (E_S^2 + 1.91 E_S E_L + 2.00 E_L^2) & k \ll k_* \\ 10.16\left(\dfrac{k}{k_*}\right)^{14} \exp\left[-2\left(\dfrac{k}{k_*}\right)^2\right] E_S^2 & k \gg k_* , \end{cases} \tag{3.24}$$

where $k_*(\Delta v)$ is defined in equation (3.20). In the inner crust of a neutron star $k_*(\Delta v) \simeq 6 \times 10^{-3} \Delta v_7^{1/2}$ fm^{-1}, where $\Delta v_7 \equiv \Delta v/(10^7$ cm s$^{-1})$. The two expressions (3.24) are shown as dashed lines in Figure 1. The production rate $\partial n_k/\partial t$ is nearly flat for $k \ll k_*$ and decreases rapidly at $k \gtrsim 3k_*$. An expression that approximates the proper behavior is

$$\frac{\partial n_k}{\partial t} \simeq \left(\frac{\partial n_k}{\partial t}\right)_0 \left\{\frac{1 + 4.456(k/k_*)^2}{1 + \exp\,[10(k/k_* - 2.6)]}\right\} , \tag{3.25}$$

where $(\partial n_k/\partial t)_0$ is the $k \ll k_*$ limit given in equation (3.24). The solid curve in Figure 1 shows this approximate expression. The coefficient of $(k/k_*)^2$ is chosen so that the power deposited per

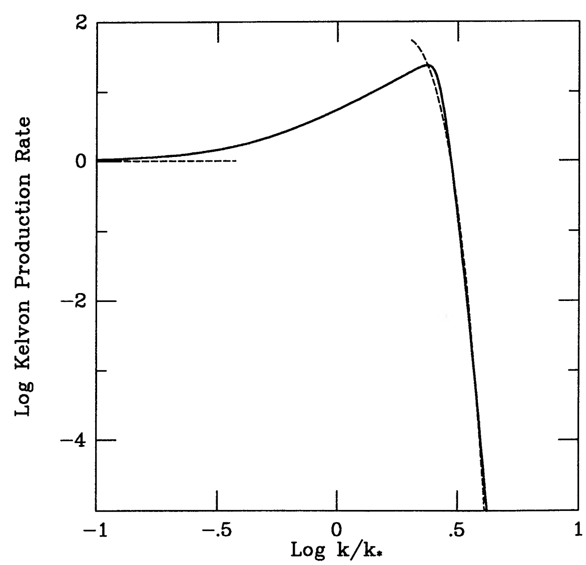

FIG. 1.—Spectrum of vortex excitations generated by a vortex line interacting with a nucleus, $(\partial n/\partial t)/(\partial n/\partial t)_0$, is shown as a function of k/k_*. Dashed lines show the limiting forms of the kelvon excitation rate (e.g. [3.24]), and the solid line gives the approximate expression (eq. [3.25]). For this figure we take $E_S \gg E_L$.

unit length,

$$p_d = \int_{-\infty}^{\infty} \hbar\omega_k \frac{\partial n_k}{\partial t} \frac{dk}{2\pi} \quad (3.26)$$

evaluated with equation (3.25) agrees with equation (3.17) for $|E_S| \gg |E_L|$, which is generally the interesting limit.

4. VORTEX DYNAMICS AND DISSIPATION

The crust rotation rates in pulsars are observed generally to decrease. To the extent that the vortex distribution is frozen into the crust, the superfluid is unable to slow down with the crust; this freezing allows the differential velocity between the crust and the superfluid to grow. If there were no forces pinning vortex lines to the crust, the lines would move with the same velocity as the superfluid. However, when a vortex line is pinned to the crust, the superfluid streams past the line, producing a Magnus force per unit length of vortex line:

$$f_M = \rho_s \boldsymbol{\kappa} \times (\boldsymbol{v}_v - \boldsymbol{v}_s) , \quad (4.1)$$

where $\boldsymbol{\kappa}$, whose magnitude is κ, is aligned with the vortex line; $\boldsymbol{v}_v - \boldsymbol{v}_s$ is the relative velocity of the vortex line with respect to the superfluid. A sufficiently large Magnus force breaks the pinning bonds and enables the vortex lines to move in the star. The characteristic relative velocity, v_B, at which vortex lines break free is found by equating the magnitude of the Magnus force with the maximum pinning force per unit length; this balance is approximately given by

$$\rho_s \kappa v_B \simeq \frac{F_{\max}}{d_p} , \quad (4.2)$$

where $F_{\max}$ is the maximum pinning force per site and d_p is the minimum distance between pinning sites on a given line. At a smaller Magnus force the line may still break free if it has enough excitation energy to overcome the potential barriers of the pinning bonds (Alpar et al. 1984; Link & Epstein 1991).

In the inner crust of neutron stars, vortex lines pin on nuclei or in the interstices between nuclei, depending on the local stellar density. In the high-density ($\gtrsim 10^{13}$ g cm^{-3}) part of the inner crust, the vortex-nucleus interaction is attractive, and the lines strongly pin on nuclei. At lower densities the interaction is repulsive; the vortex lines tend to avoid nuclei and can weakly pin to the spaces between the nuclei. We refer to these two density regimes as the *nuclear pinning* and *interstitial pinning* regions, respectively (Paper I; Link & Epstein 1991).

Table 2 lists v_B for several densities in the inner crust of a neutron star, for the full and reduced values of E_S. In the nuclear pinning region $F_{\max}$ and thus v_B are proportional to E_S (to within possible dependence of the length scale of the interaction on E_S, which we ignore here; see Link & Epstein 1991 for a more complete discussion). In the interstitial pinning region v_B is effectively independent of E_S. The abrupt change in v_B near a stellar density $\sim 8 \times 10^{12}$ g cm^{-3} marks the transition from the interstitial pinning region to the nuclear pinning region. Most models of the dynamical evolution of the superfluid in the inner crust of a neutron star predict that the relative velocity Δv of the unpinned or free vortex lines is $\sim v_B$. For velocities of this order, the condition (3.22) that the nuclear scatterings are largely independent is satisfied except at the highest densities (see Table 2).

One promising explanation for giant glitches in pulsars invokes *catastrophic unpinning* of vortex lines in some region of the inner crust (Anderson & Itoh 1975). In this model the vortex lines remain pinned until the velocity difference Δv_s between the superfluid and crust builds up to near its maximum value v_B. At some instant, a small fraction $\Phi_{\rm free}$ of the vortex lines in the inner crust are assumed to unpin by an unspecified process. After unpinning, the free vortex lines migrate outward as they transfer angular momentum from the superfluid to the solid crust.

The rate at which the glitch instability grows and the spin-up time scale for a glitch are determined by the mechanisms that transfer angular momentum from the superfluid to the solid crust. The importance of understanding the physics of the transfer time scale was underscored by the recent determination by Hamilton et al. (1989) (also see Flanagan 1989, 1990; McCulloch et al. 1990) that the spin-up time scale for a glitch in the Vela pulsar did not exceed 2 minutes. We now turn to a description of these coupling processes. First we discuss vortex motion and superfluid dynamics. After that we relate the superfluid dynamics to the dissipative mechanism derived in the previous section and consider the global behavior of the superfluid in the star.

An unpinned segment of a vortex line moves according to the dynamical equation

$$f_M + f_{\rm other} = 0 , \quad (4.3)$$

where $f_{\rm other}$ are all the forces, other than the Magnus force, that act on the line. If there are no other forces, the vortex line is swept along with the superfluid, and no angular momentum is exchanged between the superfluid and the crust. Only when there are azimuthal forces on a vortex line, which apply torques to the crust and to the superfluid, does a vortex line move in the radial direction and change the angular momentum of the superfluid and hence that of the crust.

We consider a viscous drag between the vortex line and the crust of the form

$$f_{\rm other} \to f_{\rm drag} = -\eta\, \Delta\boldsymbol{v} , \quad (4.4)$$

where η is a drag coefficient and $\Delta\boldsymbol{v}$ is the relative velocity of the vortex line through the crust. The power dissipated per length of vortex line by this drag is

$$p_d = -f_{\rm drag} \cdot \Delta\boldsymbol{v} = \eta(\Delta v)^2 . \quad (4.5)$$

Substituting equation (4.4) in the dynamical equation (4.3), one sees that the vortex motion is governed by the equation

$$\hat{\kappa} \times (\boldsymbol{v}_v - \boldsymbol{v}_s) = \tan\theta_d\, \Delta\boldsymbol{v} , \quad (4.6)$$

where $\hat{\kappa} \equiv \boldsymbol{\kappa}/\kappa$,

$$\tan\theta_d \equiv \frac{\eta}{\rho_s \kappa} , \quad (4.7)$$

and θ_d is the *dissipation angle*. As one sees from the azimuthal component of equation (4.6), the trajectory of a vortex line in a frame comoving with the crust is at an angle θ_d with respect to the superfluid velocity, that is, the radial component of the vortex velocity is

$$v_r = \Delta v \sin\theta_d . \quad (4.8)$$

The fact that the radial velocity is bounded by the magnitude of the velocity of the vortex line with respect to the crust can be understood by a simple geometric argument. A vortex reacts only to nuclei that are closer than $\sim R$, the effective nuclear radius, and each interaction can at most deflect a segment of length l_i a distance $\sim R$ in the radial direction.

The maximum radial velocity $v_{r,\max}$ due to these interactions is proportional to the product of the frequency of vortex-nucleus encounters and the maximum radial deflection. As a free vortex line of length L moves through the crystal lattice with a relative velocity Δv, it strongly interacts with $\dot{n} = \dot{N}/L \simeq 2R\,\Delta v n_N$ nuclei per unit length and time. The length of the vortex line segment deflected by each interaction cannot exceed l_i, the mean spacing between interacting nuclei along the vortex line, given by equation (3.19). The maximum value of the mean radial velocity is thus

$$v_{r,\max} \simeq \dot{n} l_i R \simeq \Delta v \ . \tag{4.9}$$

The dynamical equation (4.6) also implies that v_r varies with lag between the velocities of the crust and superfluid, $\Delta v_s \equiv |\boldsymbol{v}_s - \boldsymbol{v}_c|$, as

$$v_r = \tfrac{1}{2}\Delta v_s \sin 2\theta_d \ . \tag{4.10}$$

The lag velocity Δv between the vortex and the solid crust depends on Δv_s as

$$\Delta v = \Delta v_s \cos \theta_d \ . \tag{4.11}$$

In the absence of dissipation, $\theta_d = 0$ and $\Delta v = \Delta v_s$.

To estimate θ_d in terms of the dissipative processes discussed in § 3, we equate the dissipated powers (4.5) and (3.17) to obtain

$$\cos \theta_d = [1 + (v_*/\Delta v)^3]^{-1/2} \ . \tag{4.12}$$

This estimate for θ_d is only valid as long as Δv is not too small. Indeed, naively using equation (4.12) in equation (4.11), one finds

$$\Delta v_s = [(\Delta v)^2 + v_*^3/\Delta v]^{1/2} \ , \tag{4.13}$$

which implies that Δv_s as a function of Δv has a minimum value $2^{-1/3}v_*$. The problem is that the approximations leading to equation (4.12) break down for Δv too small, and hence θ_d too large. A complete treatment of the vortex dissipation for low velocities needs to include the effects of the vortex-nucleus interactions on the kelvon dispersion relation, as well as multiple excitation and collective processes. These topics will be treated elsewhere. The effect of such processes is to produce an upper limit to the dissipation angle $\theta_{d,\max}$. Then for $\Delta v \gg v_*$, equation (4.13) holds, while for $\Delta v \ll v_*$, one has

$$\Delta v = \cos \theta_{d,\max} \Delta v_s \ . \tag{4.14}$$

The derivation of equation (4.12) is based on two assumptions: that separate encounters of a given vortex line with different nuclei are independent, and thus $\Delta v \gg v_{\min}$ (eq. [3.22]), and that the vortex lines and nuclei are not greatly perturbed by their interactions, as underlies equation (2.5). This latter assumption does not hold for very small differential velocities for which the dissipation angle and the drag force become very large. To see how this lower limit on Δv comes about, consider the magnitude of the distortion of a vortex line due to nuclear interactions. From the dynamic equations (4.1) and (4.3), we see that the magnitude of the perturbation of the vortex velocity is $\delta v_v \sim \langle f_{\rm int}\rangle/\rho_s \kappa$ where $\langle f_{\rm int}\rangle$ is the interaction force averaged over the segment of line that is perturbed. The net distortion of the line is thus $\delta s_v \sim \delta v_v \langle t_{\rm int}\rangle$, where $\langle t_{\rm int}\rangle \sim b/\Delta v$ is the characteristic time scale for the impulse; therefore

$$\frac{\delta s_v}{b} \sim \frac{\langle f_{\rm int}\rangle}{\rho_s \kappa \Delta v} \ . \tag{4.15}$$

A necessary condition for the derivation of equation (4.12) to be valid is that the vortex displacement δs_v be small compared to the impact parameter b. This condition implies that $\Delta v \gg \langle f_{\rm int}\rangle/\rho_s \kappa \sim \delta v_v$. Since the net radial velocity v_r of the vortex line has to be less than the perturbed velocity δv_v, the derivation of equation (4.12) holds only for $\Delta v \gg v_r$ and thus $\theta_d \ll 1$ or equivalently $\Delta v \gg v_*$.

In Figure 2 we show the dependence of the radial velocity v_r on the superfluid lag velocity Δv_s obtained by taking θ_d from equations (4.11) and (4.12), but bounded from above by the illustrative value, $\theta_{d,\max} = 0.7$.

We consider now the global motion of the superfluid in the star. The angular velocity of the superfluid $\Omega_s(r)$ at a cylindrical radius r from the rotation axis is proportional to the mean density of vortex lines within this radius. If a fraction $\Phi_{\rm free}$ of the vortex lines is not pinned to the crust and is free to move radially with velocity v_r, then the average superfluid rotation slows at a rate given by

$$\frac{\dot{\Omega}_s}{\Omega_s} = \frac{\dot{N}_v}{N_v} = -\frac{2v_r \Phi_{\rm free}}{r} \ , \tag{4.16}$$

where N_v is the number of vortices interior to cylindrical radius r. The angular momentum lost by the superfluid is transferred to the crust, and the angular velocity of the crust increases according to

$$\dot{\Omega}_s I_s + \dot{\Omega}_c I_c = 0 \ , \tag{4.17}$$

where I_s is the moment of inertia of the superfluid and I_c is the moment of inertia of the crust plus that of the components that are strongly coupled to the crust. Since the liquid core of the star dynamically couples to the crust on short time scales (Alpar, Langer, & Sauls 1984; Alpar & Sauls 1988), I_c is nearly the moment of inertia of the entire star, and $I_s/I_c \sim 10^{-2}$. The spin-up time scale $t_{\rm su}$ is $\Delta\Omega_c/\dot{\Omega}_c$, where $\Delta\Omega_c$ is the angular velocity change of the crust of a neutron star during the spin-up phase of a pulsar glitch. Using equations (4.10), (4.16), (4.17), and writing $\Delta v_s = (\Omega_s - \Omega_c)r$, we find

$$t_{\rm su} = \frac{I_c \Delta\Omega_c}{I_s(\Omega_s - \Omega_c)\Phi_{\rm free}} [\Omega_s \sin 2\theta_d]^{-1} \ . \tag{4.18}$$

The numerator of the fraction is the amount of angular momentum imparted to the crust, and the denominator is the maximum angular momentum available to be extracted from the superfluid when a fraction $\Phi_{\rm free}$ of the vortex lines move

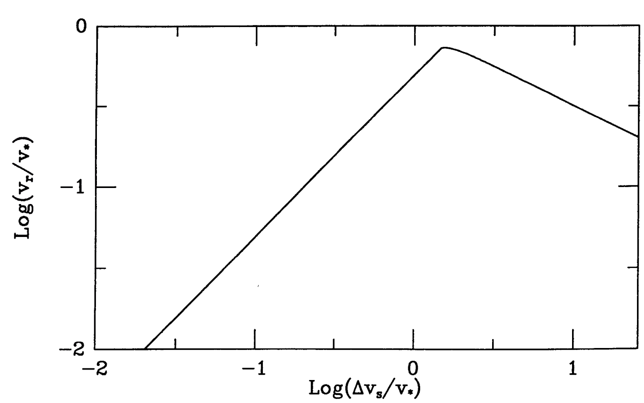

FIG. 2.—Radial velocity of a vortex line as a function of the relative velocity of the superfluid and the crust. Maximum dissipation angle is taken for the figure to be 0.7.

outward. The first term in equation (4.18) is thus less than unity, so that

$$t_{\rm su} \lesssim \frac{1}{\Omega_s \sin 2\theta_d} . \tag{4.19}$$

We expect the initial value of $\Omega_s - \Omega_c$ to be comparable to the maximum value v_B/R_*, where R_* is the stellar radius.

For $v_B \gtrsim v_*$ we obtain the spin-up time scale using equation (4.12) in equation (4.19),

$$t_{\rm su} \lesssim \frac{(v_B/v_*)^{3/2}}{2\Omega_s} . \tag{4.20}$$

For smaller v_B the maximum dissipation angle is reached, and

$$t_{\rm su} \lesssim (\Omega_s)^{-1} . \tag{4.21}$$

Among the entries in Table 2 the largest value of v_B/v_* is ~ 85 corresponding to an upper limit on the spin-up time scale of $t_{\rm su} \lesssim 60P$, where P is the rotation period.

5. THE 1988 DECEMBER 24 GLITCH IN THE VELA PULSAR

Only one giant pulsar glitch has been observed during the spin-up phase, the 1988 December 24 glitch of the Vela pulsar (Hamilton et al. 1989; McCulloch et al. 1990; Flanagan 1989, 1990). The change in the angular velocity of the crust was $\Delta\Omega \simeq 1.3 \times 10^{-4}\ {\rm s}^{-1}$, and the spin-up time was observed to be less than 2 minutes. Previously published superfluid dissipation processes (Feibelman 1971; Bildsten & Epstein 1989; Jones 1990) give spin-up time scales much greater than 2 minutes. The spin-up time scale for the nuclear scattering process considered here is $\lesssim 5$ s for the Vela pulsar, more than adequate for explaining the required rate of angular momentum transfer from the superfluid to the crust. However, within the *catastrophic unpinning* model for glitches, the instability that forces many vortex lines to unpin rapidly remains an important unanswered question.

The total number of pinned vortex lines in the Vela pulsar is $\sim 10^{15}$, and a fraction $\Phi_{\rm free}$ of these unpin during a giant glitch. A lower limit on $\Phi_{\rm free}$ can be obtained by considering the angular momentum $I_c\,\Delta\Omega_c$ transferred from the superfluid to the crust during a glitch. Since the maximum amount of angular momentum that the superfluid can lose is $\sim I_s\,\Phi_{\rm free}\,|\Omega_s - \Omega_c|$, equating angular momentum loss and gain gives $\Phi_{\rm free} \gtrsim I_c\,\Delta\Omega_c/I_s\,|\Omega_s - \Omega_c|$. To obtain a numerical estimate we take $|\Omega_s - \Omega_c| \simeq v_B/R_*$ which gives

$$\Phi_{\rm free} \gtrsim 10^{-3}\left(\frac{I_c}{10^2 I_s}\right)\left(\frac{\Delta\Omega_c}{10^{-4}\ {\rm s}^{-1}}\right)\left(\frac{R_*}{10^6\ {\rm cm}}\right)\left(\frac{v_B}{10^7\ {\rm cm\ s}^{-1}}\right)^{-1} . \tag{5.1}$$

The ratio I_s/I_c depends sensitively on the equation of state. For a 1.4 $M_\odot$ star the "stiff" Pandharipande & Smith (1975) equation of state gives $I_s/I_c \sim 0.2$ for the nuclear pinning region and ~ 0.003 for the interstitial pinning region. For the "soft" Baym, Pethick, & Sutherland (1971) equation of state I_s/I_c is ~ 0.005 for the nuclear pinning region and $\sim 10^{-4}$ for the interstitial pinning region. If a giant glitch originates in the nuclear pinning region of the inner crust where $v_B \sim 10^7$ cm s^{-1}, only a very small fraction, of order 10^{-3}, of the vortex lines need to be involved. On the other hand, if the glitch originates in the interstitial pinning region, where $v_B \sim 10^5$ cm s^{-1}, then ~ 0.3 of the vortex lines in this region would have to unpin catastrophically for a star with a stiff equation of state, and a giant glitch would not be possible if the equation of state were much softer.

This work was carried out under the auspices of the Department of Energy and supported in part by NSF grant DMR 88-18713. We have had useful discussions with Ali Alpar, David Pines, Mal Ruderman, and Noriaki Shibazaki about the observational consequences of large pinning strengths, and with Edouard Sonin about limits on $f_{\rm drag}$.

APPENDIX A

VORTEX EXCITATIONS

Consider a vortex line segment of length L oriented along the z-axis of a Cartesian coordinate system. Let the vortex line have a small displacement $\boldsymbol{\epsilon}(z, t)$ given by equation (3.1), and a perturbation in its velocity $\boldsymbol{v}_v(z, t) = \partial\boldsymbol{\epsilon}(z, t)/\partial t$. We take the unperturbed vortex line to be at rest in the superfluid and neglect vortex-vortex interactions and Coriolis effects. For a tensile force $T\partial^2\boldsymbol{\epsilon}(z, t)/\partial z^2$, the dynamical equation of the line (cf. eqs. [4.1] and [4.3]) becomes

$$\rho_s \boldsymbol{\kappa} \times \frac{\partial\boldsymbol{\epsilon}(z, t)}{\partial t} + T\,\frac{\partial^2\boldsymbol{\epsilon}(z, t)}{\partial z^2} = 0 , \tag{A1}$$

where ρ_s is the superfluid mass density and $\boldsymbol{\kappa} = (\pi\hbar/m_n)\hat{z}$.

We define complex coordinates ϵ_+ and ϵ_- by

$$\epsilon_+(z, t) = \boldsymbol{\lambda}^* \cdot \boldsymbol{\epsilon}(z, t) , \qquad \epsilon_-(z, t) = \boldsymbol{\lambda} \cdot \boldsymbol{\epsilon}(z, t) , \tag{A2}$$

where $\boldsymbol{\lambda}$ is the complex unit polarization vector (3.6). The displacement of the vortex line is thus

$$\boldsymbol{\epsilon}(z, t) = [\epsilon_+(z, t)\boldsymbol{\lambda} + \epsilon_-(z, t)\boldsymbol{\lambda}^*] . \tag{A3}$$

In terms of $\epsilon_\pm(z, t)$ the dynamic equation (A1) is

$$i\rho_s \kappa\, \frac{\partial\epsilon_\pm(z, t)}{\partial t} \pm T\,\frac{\partial^2\epsilon_\pm(z, t)}{\partial z^2} = 0 . \tag{A4}$$

In (k, t)-coordinates equation (A4) is

$$\frac{\partial \epsilon_{\pm}(k, t)}{\partial t} \pm i\omega_k \epsilon_{\pm}(k, t) = 0 , \tag{A5}$$

where

$$\omega_k \equiv \frac{Tk^2}{\rho_s \kappa} = \frac{\hbar k^2}{2\mu} , \tag{A6}$$

and

$$\mu \equiv \rho_s \kappa \hbar / 2T . \tag{A7}$$

Coriolis effects would add a term $2\Omega_s$ to the frequency (A6), where Ω_s is the superfluid rotational velocity.

In (k, ω)-coordinates (A4) is

$$(\omega \mp \omega_k)\epsilon_{\pm}(k, \omega) = 0 . \tag{A8}$$

Equations (A5) and (A8) are actually more general than (A4) because in the latter T can be a function of k; hereafter, when working in k-space we consider T and μ to depend on k. From equation (A8) we see that the eigenfrequencies of the lines are ω_k for $\epsilon_+(k, \omega)$ and $-\omega_k$ for $\epsilon_-(k, \omega)$. These two modes, simply complex conjugates of each other, represent only one independent solution. Since the dynamical equation is only first order in the time derivative, it has only one solution, the well-known vortex wave (Thomson 1880; Fetter 1967); the displacement $\boldsymbol{\epsilon}(z, t)$ rotates in the clockwise direction relative to $\boldsymbol{\kappa}$, whereas the fluid circulates around the vortex line in the opposite direction.

For perturbations of wavenumber k, the tension is

$$T = \frac{\rho_s \kappa^2}{2} \Lambda(k) , \tag{A9}$$

which gives

$$\mu = \frac{m_n}{\pi \Lambda(k)} . \tag{A10}$$

The factor Λ depends logarithmically on the wavenumber k. If the vortex lines are widely spaced compared to the radius of the vortex core ξ, and if $k\xi \ll 1$, then (Thomson 1880; Fetter 1967)

$$T_k = \frac{\rho_s \kappa^2}{4\pi} (a - \ln k\xi) , \tag{A11}$$

where $a \simeq 0.116$ for a vortex line with a hollow core. This form for the tension yields a vanishing group velocity at $k = k_0 \simeq 0.68/\xi$; the classical vortex wave theory is valid only for $k \ll k_0$.

The energy of a perturbation in a vortex line is

$$\begin{aligned} E(t) &= \frac{1}{2} \int_{-L/2}^{L/2} T \left| \frac{\partial \boldsymbol{\epsilon}(z, t)}{\partial z} \right|^2 dz \\ &= \frac{1}{2L} \sum_k Tk^2 [\epsilon_x(k, t)\epsilon_x(-k, t) + \epsilon_y(k, t)\epsilon_y(-k, t)] \\ &= \frac{1}{2L} \sum_k Tk^2 |\boldsymbol{\epsilon}(k, t)|^2 . \end{aligned} \tag{A12}$$

Vortex wave excitations are, in fact, quantized; in this paper we refer to quantized vortex oscillations as kelvons. To derive the properties of kelvons, we first express $E(t)$ as a Hamiltonian $H(q_k, p_k)$, where q_k and p_k are conjugate coordinates and momenta. With the definitions

$$q_k \equiv \left(\frac{\rho_s \kappa}{L}\right)^{1/2} \epsilon_x(k, t) , \qquad p_k \equiv \left(\frac{\rho_s \kappa}{L}\right)^{1/2} \epsilon_y(-k, t) , \tag{A13}$$

the energy (A12) can be written as a Hamiltonian

$$H = \tfrac{1}{2} \sum_k \omega_k (q_k q_{-k} + p_k p_{-k}) , \tag{A14}$$

so that Hamilton's equations,

$$\frac{\partial H}{\partial q_k} = -\dot{p}_k , \qquad \frac{\partial H}{\partial p_k} = \dot{q}_k , \tag{A15}$$

give the equations of motion (A5). Quantum mechanically the operators q_k and p_k as operators obey the commutation relations

$$[q_k, p_{k'}] = i\hbar\delta_{k,k'} . \tag{A16}$$

We now introduce kelvon creation and annihilation operators, $a_k^\dagger$ and a_k.

$$a_k^\dagger = \frac{1}{\sqrt{2\hbar}}[q_{-k} - ip_k] , \qquad a_k = \frac{1}{\sqrt{2\hbar}}[q_k + ip_{-k}] . \tag{A17}$$

These operators satisfy the Bose commutation relations:

$$[a_k, a_{k'}^\dagger] = \delta_{k,k'} , \qquad [a_k, a_{k'}] = [a_k^\dagger, a_{k'}^\dagger] = 0 . \tag{A18}$$

Inversion of equation (A17) gives

$$q_k = \sqrt{\frac{\hbar}{2}}[a_k + a_{-k}^\dagger], \qquad p_k = i\sqrt{\frac{\hbar}{2}}[a_k^\dagger - a_{-k}] . \tag{A19}$$

Substituting these relations into the Hamiltonian (A14) formally yields $H = \sum_k \hbar\omega_k(a_k^\dagger a_k + \frac{1}{2})$. Since the Hamiltonian only describes excitations above the ground state of the system, not the ground state itself, we drop the zero-point term, and have

$$H = \sum_k \hbar\omega_k a_k^\dagger a_k . \tag{A20}$$

Since $a_k^\dagger a_k$ is the number operator with eigenvalues $n_k = 0, 1, 2, \ldots$, the energy levels for a mode of wavenumber k are $n_k \hbar\omega_k$.

Using the definitions of the conjugate coordinates and the creation and annihilation operators (A13) and (A17), we express the vortex displacement (A3) as

$$\boldsymbol{\epsilon}(z, t) = \left(\frac{\hbar}{\rho_s \kappa L}\right)^{1/2} \sum_k [a_k e^{ikz}\boldsymbol{\lambda} + a_k^\dagger e^{-ikz}\boldsymbol{\lambda}^*] . \tag{A21}$$

From equation (A21) we find that the mean square amplitude of a kelvon of wavevector k is

$$\langle\epsilon_k^2\rangle = 2\hbar/\rho_s \kappa L = 2m_n/\pi\rho_s L . \tag{A22}$$

For neutron star values, $L \sim 10^6$ cm and $\rho_s \sim 10^{13}$ g cm^{-3}, the root mean square amplitude is $\sim 3 \times 10^{-22}$ cm.

From equation (A21) we find the equal time commutation relations

$$[\epsilon_x(z), \epsilon_x(z')] = [\epsilon_y(z), \epsilon_y(z')] = 0 , \qquad [\epsilon_x(z), \epsilon_y(z')] = \frac{2\pi i\hbar}{\rho_s \kappa} . \tag{A23}$$

The failure of ϵ_x and ϵ_y to commute arises from the implicit assumption that the vortex lines have no inertial mass. In the presence of an inertial mass, ρ^* per unit length, the lines also have a high-frequency mode, $\omega^* \simeq (T/\rho^*)^{1/2}k$, which is not included in the sum (A21) over normal modes (Baym & Chandler 1983). With this mode taken into account, all components of the vortex displacement commute at equal times. In effect, in writing equation (A21) we are averaging over the high-frequency cycloidal motion; the time-averaged displacements obey nonzero commutation relations. The situation is entirely analogous to the quantum mechanics of guiding center coordinates in the motion of a charged particle in a large magnetic field (Baym & Epstein 1992).

The angular momentum of a kelvon can be found by considering a vortex in a cylinder of superfluid of radius R_c and length L. Let the unperturbed vortex be aligned with the cylinder and offset from the axis by $\boldsymbol{r}_0$. The position of points along the excited vortex are given by

$$\boldsymbol{r}_v(z, t) = \boldsymbol{r}_0 + \boldsymbol{\epsilon}(z, t) . \tag{A24}$$

The component of the angular momentum along the cylinder axis of the fluid in the cylinder is

$$J_z = \int dz\, d^2r \rho_s(\boldsymbol{r} \times \boldsymbol{v})_z = \rho_s \int_{-L/2}^{L/2} \int_0^{R_c} (2\pi r v_\phi) r\, dr\, dz . \tag{A25}$$

Since the circulation $2\pi r v_\phi$ in the integrand is a step function, $\kappa\Theta(r - r_v)$, we have

$$J_z = \frac{\rho_s \kappa}{2} \int [R_c^2 - r_v(z, t)^2] dz . \tag{A26}$$

We substitute equations (A21) and (A24) into this expression and separate the results into a term J_0 that gives the contribution from the straight vortex line, and a term ΔJ that contains the contributions from the oscillatory perturbations. The angular momentum term for the straight vortex is

$$J_0 = \frac{\rho_s \kappa L}{2} [R_c^2 - (r_0 + \epsilon_0)^2] , \tag{A27}$$

where ϵ_0 is the $k = 0$ perturbation of the line. The perturbation ϵ_0 is simply a translation of the vortex, determined by global energy and momentum conservation, and is not a kelvon excitation. The component ΔJ has terms linear and quadratic in ϵ_k. Upon integrating over z the linear terms vanish, leaving

$$\Delta J = -\frac{\rho_s \kappa}{2} \int |\epsilon(z, t) - \epsilon_0|^2 \, dz \to -\hbar \sum_{k \neq 0} a_k^\dagger a_k \,, \tag{A28}$$

where we again drop the zero-point term. As we see, each kelvon carries an angular momentum $-\hbar$.

When a kelvon is generated, the vortex line must undergo a uniform displacement ϵ_0 in order to conserve energy and angular momentum globally. In the creation of a kelvon of wavenumber k, the kinetic energy of the superfluid decreases by $j_k \Omega_s$, where j_k is the angular momentum transferred from the superfluid to the crust of a neutron star in the creation of the kelvon, and Ω_s is the angular velocity of the superfluid in the neighborhood of the vortex line. The energy of the crust increases by $j_k \Omega_c$, where Ω_c is the angular velocity of the crust. The net loss in rotational kinetic energy goes into the kelvon excitation: $\hbar\omega_k = j_k(\Omega_s - \Omega_c)$, so that

$$j_k = \frac{\hbar\omega_k}{\Omega_s - \Omega_c} \,. \tag{A29}$$

The characteristic kelvon frequency in neutron stars, $\omega_k \sim 10^{17}\ \mathrm{s}^{-1}$ is many orders of greater than the macroscopic rotation rates Ω_s or Ω_c. The angular momentum change j_k induced by the generation of a kelvon is thus huge compared to the angular momentum $-\hbar$ associated with the oscillations of the vortex line; most of the change results from the small shift, ϵ_0, of the mean position of the vortex line. To estimate the magnitude of ϵ_0, we equate the term linear in ϵ_0 in the angular momentum (A27) with j_k, to find

$$\epsilon_0 = \frac{\langle \epsilon_k^2 \rangle}{2r_0} \frac{\omega_k}{\Omega_s - \Omega_c} \,, \tag{A30}$$

where $\langle \epsilon_k^2 \rangle$ is the mean square amplitude of a kelvon (eq. [A22]). For characteristic neutron star values, $r_0 \sim L \sim 10^6$ cm and $\rho_s \sim 10^{13}\ \mathrm{g\ cm}^{-3}$, the ratio of the $k = 0$ displacement to the root mean square kelvon displacement is

$$\frac{\epsilon_0}{\langle \epsilon_k^2 \rangle^{1/2}} \simeq 10^{-28} \frac{\omega_k}{\Omega_s - \Omega_c} \,. \tag{A31}$$

This displacement is extremely small, but the sum of these small shifts produces the net radial velocity of a vortex line given by equation (4.10).

APPENDIX B

FOURIER TRANSFORM $f_+(k, \omega_k)$

The transform of the force component $f_+(k, t)$ given by equations (2.6) and (3.12) is

$$f_+(k, \omega_k) = \frac{\sqrt{2}}{R} \int_{-\infty}^{\infty} (\tau + i\tau_b) \left[\frac{4E_S}{(1 + \tau^2 + \tau_b^2)^5} + \frac{E_L}{(1 + \tau^2 + \tau_b^2)^2} \right] e^{i\omega_k t} \, dt \int_{-\infty}^{\infty} \phi(z, t) e^{-ikz} \, dz \,, \tag{B1}$$

where $\tau = \Delta v t / R$ and here we write ϕ as an explicit function of t. We change the integration variable to τ so that $f_+(k, \omega_k)$ becomes

$$f_+(k, \omega_k) = \frac{\sqrt{2}}{\Delta v} \int_{-\infty}^{\infty} (\tau + i\tau_b) \left[\frac{4E_S}{(1 + \tau^2 + \tau_b^2)^5} + \frac{E_L}{(1 + \tau^2 + \tau_b^2)^2} \right] \phi(k, t) \exp\left(\frac{i\omega_k R\tau}{\Delta v} \right) d\tau \,. \tag{B2}$$

The function $\phi(z, t)$ defines how the force $\boldsymbol{F}_{\mathrm{int}}$ is distributed along the vortex line. As we show below, the exact form of $\phi(z, t)$ is unimportant because the range over which $\boldsymbol{F}_{\mathrm{int}}$ acts is small compared to the wavelengths of the modes that are excited; in effect, ϕ can be approximated by a delta function: $\phi(z, t) \to \delta(z)$, or $\phi(k, t) \to 1$. To illustrate how the range of ϕ enters into the computation of E_{scatt}, we take ϕ to have the simple form

$$\phi(z, t) = \frac{1}{W\sqrt{\pi}} \exp\left(-\frac{z^2}{W^2} \right) , \tag{B3}$$

where $W(\tau)$ is the characteristic range of $\phi(z, t)$. The transform $\phi(k, t)$ is

$$\phi(k, t) = \exp\left(-\frac{k^2 W^2}{4} \right) , \tag{B4}$$

and $f_+(k, \omega_k)$ is

$$f_+(k, \omega_k) = \frac{\sqrt{2}}{\Delta v} \int_{-\infty}^{\infty} (\tau + i\tau_b) \left[\frac{4E_S}{(1 + \tau^2 + \tau_b^2)^5} + \frac{E_L}{(1 + \tau^2 + \tau_b^2)^2} \right] \exp\left(\frac{i\omega_k R}{\Delta v} \tau - \frac{k^2 W^2}{4} \right) d\tau \,. \tag{B5}$$

If $W(\tau)$ does not grow too quickly for $|\tau| \to \infty$ in the upper-half of the complex τ-plane, then we can solve equation (B5) by contour integration. We proceed by defining integrals $f_a(k, \omega_k)$ and $f_b(k, \omega_k)$:

$$f_a(k, \omega_k) \equiv \int_{-\infty}^{\infty} \frac{\tau}{(1 + \tau^2 + \tau_b^2)} \exp\left(\frac{i\omega_k R}{\Delta v}\tau - \frac{k^2 W^2}{4}\right) d\tau , \tag{B6}$$

$$f_b(k, \omega_k) \equiv \int_{-\infty}^{\infty} \frac{1}{(1 + \tau^2 + \tau_b^2)} \exp\left(\frac{i\omega_k R}{\Delta v}\tau - \frac{k^2 W^2}{4}\right) d\tau . \tag{B7}$$

The transform $f_+(k, \omega_k)$ can be obtained by differentiating the integrals $f_a(k, \omega_k)$ and $f_b(k, \omega_k)$ with respect to τ_b and adding the results together with the appropriate weights. The integrands of $f_a(k, \omega_k)$ and $f_b(k, \omega_k)$ have poles at $\tau = \pm i(1 + \tau_b^2)^{1/2}$. Evaluating $f_a(k, \omega_k)$ and $f_b(k, \omega_k)$ with contour integrals closed in the upper half-plane gives

$$f_a(k, \omega_k) = i\pi \exp\left[-\frac{k^2 R^2}{2}\left(\hbar \frac{\sqrt{1 + \tau_b^2}}{\mu \Delta v R} - \frac{W_{\rm res}^2}{2R^2}\right)\right], \tag{B8}$$

and

$$f_b(k, \omega_k) = \frac{\pi}{\sqrt{1 + \tau_b^2}} \exp\left[-\frac{k^2 R^2}{2}\left(\frac{\hbar\sqrt{1 + \tau_b^2}}{\mu \Delta v R} - \frac{W_{\rm res}^2}{2R^2}\right)\right], \tag{B9}$$

where $W_{\rm res}$ is $W(\tau)$ evaluated at the pole in the upper half-plane, $W_{\rm res} = W[i(1 + \tau_b^2)^{1/2}]$.

When $\tau \sim \tau_b$ the length scale $W(\tau)$ is of the order of the nucleus-vortex separation,

$$W(\tau) \simeq R(\tau^2 + \tau_b^2)^{1/2} , \tag{B10}$$

and

$$W_{\rm res}^2 \simeq -R^2 . \tag{B11}$$

With this estimate we see that the second term in the parentheses in equations (B8) and (B9) is negligible compared to the first if

$$\mu \Delta v R \ll \hbar . \tag{B12}$$

This condition corresponds to

$$\Delta v \ll 1.7 \times 10^9 \left(\frac{\Lambda}{3}\right)\left(\frac{R}{7\ \rm fm}\right)^{-1} \rm cm\ s^{-1} . \tag{B13}$$

Since the maximum values of Δv expected in a neutron star are of the order of $v_B \lesssim 10^8$ cm s^{-1} (see Table 2), the contribution of the $W_{\rm res}$ is not very important. We do not retain this term in the following, a step equivalent to taking $\phi(z, t) \sim \delta(z)$.

The transform $f_+(k, \omega_k)$ is now obtained by differentiating $f_a(k, \omega_k)$ and $f_b(k, \omega_k)$ with respect to τ_b and creating the appropriate sum of these results. Using MACSYMA we obtain

$$\begin{aligned} f_+(k, \omega_k) = \frac{\pi i}{\Delta v} \exp(-K^2 T_b)\Bigg\{&\frac{E_S}{48 T_b^9}[105\tau_b + 15K^2(T_b^2 + 7\tau_b T_b) + 15(T_b^3 + 3\tau_b T_b^2) \\ &+ 2K^6(3T_b^4 + 5\tau_b T_b^3) + K^8(T_b^5 + \tau_b T_b^4)] + \frac{E_L}{T_b^3}[\tau_b + K^2(T_b^2 + \tau_b T_b)]\Bigg\} , \end{aligned} \tag{B14}$$

where $T_b \equiv (1 + \tau_b^2)^{1/2}$, $K \equiv k/k_* = (\omega_k R/\Delta v)^{1/2}$, and $k_* \equiv (2\mu \Delta v/\hbar R)^{1/2}$.

APPENDIX C

CLASSICAL DERIVATION OF THE VORTEX-NUCLEUS INTERACTION

The dynamical equation for the vortex perturbation (A1) including the interaction force (2.6) is

$$\rho_s \boldsymbol{\kappa} \times \frac{\partial \boldsymbol{\epsilon}(z, t)}{\partial t} + T \frac{\partial^2 \boldsymbol{\epsilon}(z, t)}{\partial z^2} + \boldsymbol{f}_{\rm int}(z, t) = 0 . \tag{C1}$$

This equation can be written in terms of the complex amplitudes $\epsilon_\pm$ and $f_\pm$ given by equations (A2) and (3.12):

$$\pm i\rho_s \kappa \frac{\partial \epsilon_\pm(z, t)}{\partial t} + T \frac{\partial^2 \epsilon_\pm(z, t)}{\partial z^2} + f_\pm(z, t) = 0 . \tag{C2}$$

Fourier transforming the equation for ϵ_+ one has

$$(\rho_s \kappa \omega - k^2 T)\epsilon_+(k, \omega) = f_+(k, \omega) . \tag{C3}$$

Then Fourier transforming in time and using the definition (A6) for ω_k we obtain

$$\epsilon_+(k, t) = \frac{1}{\rho_s \kappa} \int_{-\infty}^{\infty} \frac{f_+(k, \omega) e^{-i\omega t}}{(\omega - \omega_k + i\eta)} \frac{d\omega}{2\pi} . \tag{C4}$$

Here we introduce an infinitesimal imaginary term $i\eta$ to ensure causality. In terms of $f_+(k, t')$ we obtain

$$\epsilon_+(k, t) = \frac{1}{\rho_s \kappa} \int_{-\infty}^{\infty} \int_{-\infty}^{\infty} \frac{f_+(k, t') e^{-i\omega(t-t')}}{[\omega - \omega_k + i\eta]} \frac{d\omega}{2\pi} dt' . \tag{C5}$$

Closing the contour of the ω-integral in the upper (for $t < t'$) and lower (for $t > t'$) half-planes, one has

$$\epsilon_+(k, t) = \frac{1}{i\rho_s \kappa} e^{-i\omega_k t} \int_{-\infty}^{t} f_+(k, t') e^{i\omega_k t'} dt' . \tag{C6}$$

Long after the vortex-nucleus interaction, we can let $t \to \infty$ so that

$$\lim_{t \to \infty} \epsilon_+(k, t) e^{i\omega_k t} = \frac{1}{i\rho_s \kappa} f_+(k, \omega_k) . \tag{C7}$$

Evaluating $\epsilon_-(k, t)$ gives $\epsilon_-(k, t) = \epsilon_+^*(k, t)$ so that the energy (eq. [A12]) deposited in perturbations of the line by a single scattering is

$$E_{\mathrm{scatt}}(\tau_b) = \lim_{t \to \infty} \frac{1}{2L} \sum_k T k^2 |\epsilon(k, t)|^2 = \frac{\hbar}{2\rho_s \kappa \mu L} \sum_k k^2 |f_+(k, \omega_k)|^2 \tag{C8}$$

in agreement with equation (3.14).

REFERENCES

Alpar, M. A. 1984, ApJ, 213, 527
Alpar, M. A., Anderson, P. W., Pines, D., & Shaham, J. 1984, ApJ, 276, 325
Alpar, M. A., Langer, S. A., & Sauls, J. A. 1984, ApJ, 282, 533
Alpar, M. A., & Sauls, J. A. 1988, ApJ, 327, 723
Anderson, P. W., & Itoh, N. 1975, Nature, 226, 25
Baym, G., & Chandler, E. 1983, J. Low Temp. Phys., 50, 57
Baym, G., & Epstein, R. I. 1992, in preparation
Baym, G., Pethick, C., & Sutherland, P. 1971, ApJ, 170, 299
Bildsten, L., & Epstein, R. I. 1989, ApJ, 342, 951
Chandler, E., & Baym, G. 1986, J. Low Temp. Phys., 62, 119
Epstein, R. I., & Baym, G. 1988, ApJ, 328, 680 (Paper I)
Feibelman, P. J. 1971, Phys. Rev. D, 4, 1589
Fetter, A. L. 1967, Phys. Rev., 162, 143
Flanagan, C. 1989, IAU Circ., No. 4695
———. 1990, Nature, 345, 416
Hamilton, P. A., King, E. A., & McCulloch, P. M. 1989, IAU Circ., No. 4708
Jones, P. B. 1990, MNRAS, 243, 257
Link, B., & Epstein, R. I. 1991, ApJ, 373, 592
Manchester, R. N., & Taylor, J. H. 1977, Pulsars (San Francisco: Freeman)
McCulloch, P. M., Hamilton, P. A., McConnell, D., & King, E. A. 1990, Nature, 346, 822
Negele, J. W., & Vautherin, D. 1973, Nucl. Phys. A, 207, 298
Pandharipande, V. R., & Smith, R. A. 1975, Nucl. Phys. A, 237, 507
Shibazaki, N., & Lamb, F. K. 1989, ApJ, 346, 808
Thomson, W. (Lord Kelvin). 1880, Phil. Mag., 10, 155
Tkachenko, V. K. 1965, Zh. Eksper. Teor. et Fiz., 49, 1875 (Soviet Phys.—JETP, 22, 1282 [1966])
———. 1966, Zh. Eksper. Theoret. Fiz., 50, 1573 (Soviet Phys.—JETP, 23, 1049 [1966])
———. 1969, Zh. Eksper. Theoret. Fiz., 56, 1763 (Soviet Phys.—JETP 29, 945 [1969])